A Study of Melt Density of Flowing Linear Polyethylene

ALFRED RUDIN and RONG-JONG CHANG, *Department of Chemical Engineering, University of Waterloo, Waterloo, Ontario, Canada*

Synopsis

Linear polyethylene was extruded from a capillary rheometer with the driving piston operated at fixed speed and at fixed pressure. Apparent viscosity and melt density were measured in both extrusion modes. Apparent density decreased at shear rates approaching the melt fracture region in fixed piston-speed operation. Flow of other polymer melts was essentially incompressible in fixed piston-speed operation, and all polymers exhibited incompressible flow in fixed-pressure extrusion. The oscillating portion of the flow curve of linear polyethylene reflects alternating periods in which the polymer exits faster and slower than the rate at which the advancing piston clears the rheometer reservoir. Linear polyethylene behaves differently from most other polymers in fixed piston-speed extrusion and during melt fracture because of the existence of a more extensive entanglement network in the melt. It is suggested that melt fracture in general results from a tensile failure of the entanglement network, which may occur at the die inlet and in the orifice.

INTRODUCTION

This article is an extension of earlier work[1] in this laboratory in which the density of thermoplastic melts was studied under conditions of flow from a reservoir into a capillary orifice. The earlier study employed a novel controlled-speed, piston-driven capillary rheometer with which it was possible to measure polymer pressure near the orifice entrance as well as the mass of material extruded per unit of volume of the reservoir cleared by the advancing piston. Simultaneous measurements were made of apparent values of shear stress, shear rate, and polymer melt density. These parameters are termed apparent because the rheological data measured were not corrected to true values at the orifice wall and because the density estimates were obtained by equating the volume of melt corresponding to a given mass of polymer to the corresponding product of piston travel and reservoir cross-sectional area.

Melt density values obtained at low shear rates agreed with those reported in the literature from measurements on static samples of the same polymers. This was as expected, in view of other data reported earlier with a similar, deadweight-driven apparatus.[2–4] At higher shear rates, however, a linear polyethylene exhibited a significant shear rate-dependent density decrease. This dilation was attributed to the triaxial action of normal stresses generated during flow of the polymer from the reservoir into the narrower orifice.

Further (unpublished) studies with the same rheometer and other polymers have failed to detect any significant density decreases during flow at higher shear rates. These other polymers also differ from linear polyethylene in their ostensible behavior during melt fracture, where this term refers to a gross extrudate deformation exhibited by polymer solutions and melts flowing through orifices

Journal of Applied Polymer Science, Vol. 22, 781–799 (1978)

0021-8995/78/0022-0781$01.00

at rates greater than certain critical values.[5–8] Early work identified the die inlet region as the site of one type of instability which is called inlet fracture or elastic melt fracture and is the primary instability in the flow of branched polyethylenes, polystyrene, polypropylene, and other polymers.[9–11] There is general but not universal agreement that this flow instability is elastic in nature.

The capillary extrusion of linear polyethylene and of certain other polymers of lesser commercial importance differ ostensibly from the behavior mentioned above in that the shear rate–shear stress curve is marked by a discontinuity and hysteresis loops.[12,13] The usual view of this instability involves adhesive failure at the die wall–polymer interface with a resulting transition from laminar to plug flow.[13,14] This instability has been termed land fracture.[6]

Our earlier study[1] of effects of shear rate on polymer melt density was pursued further in the work reported here. The controlled-speed piston rheometer was modified to permit operation at controlled pressure, and the flow of linear polyethylene at shear rates below the instability region was compared in constant piston-speed and constant-pressure modes of extrusion. An explanation is offered for the differences which were observed. Experiments were conducted in the melt fracture regimes in both modes of extrusion. the results of this work suggest that both inlet and land fracture are triggered by the same mechanism, and detailed comments are offered on the mechanism of the melt fracture in general and of linear polyethylene in particular.

EXPERIMENTAL

Two piston rheometers were used in this work. Both types permit simultaneous measurements of apparent values of shear stress, shear rate, and polymer melt density. One unit was operated with the piston driven at fixed rates. This is as described by Rudin and Vlasschaert.[1] The reservoir in both units was 12 in. long, with a 1-in. diameter. Reservoir diameters at operating temperatures were measured with a vernier bore gauge. Piston movement was registered as described before[1] with a machinist's dial gauge activated by a rigid arm attached to the moving piston. The dial gauge reading was made visible at the level of the bottom of the rheometer through reflection in two mirrors. The operator could thus time the rate of piston movement and cut extrudates at the die exit face at appropriate intervals, for subsequent weighings.

The capillary orifices were drilled, honed dies with flat (180° included angle) entries. Die material was tool steel, unless otherwise noted. Orifice length and diameter were measured at room temperature, before the capillaries were used, with a micrometer and dial gauge, respectively. Dies were cleaned before each experiment by flushing with new polymer extruded from the reservoir. A transducer located about 1 in. above the bottom of the orifice measured pressure in the melt.

The second rheometer type differed from the first only in that the piston was driven at constant pressure rather than fixed speed. Figure 1 is a schematic of this apparatus. This rheometer uses compressed nitrogen supplied from a regulated cylinder to produce a constant pressure on one side of the flexible barrier in a bladder-type accumulator. The pressure train on the other side of the accumulator was filled with hydraulic fluid. The accumulator acts to transfer the applied gas pressure to the hydraulic oil which pushes a piston down through

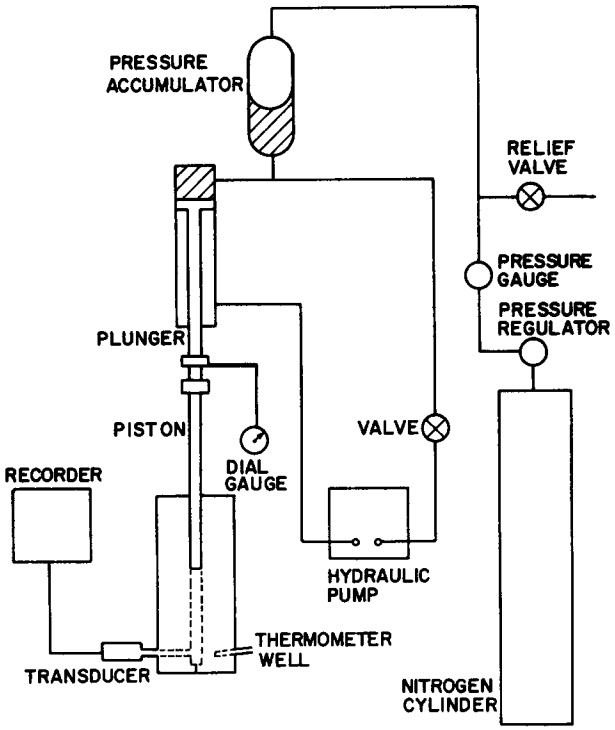

Fig. 1. Schematic of constant pressure extrusion rheometer.

a hydraulic cylinder. The rheometer piston is clamped to the end of the plunger. A hydraulic pump with a four-way valve connected to the top and bottom parts of the hydraulic cylinder serves to retract the piston and fill the accumulator with oil, as needed.

The piston, reservoir, and orifices used in the constant-pressure rheometer are the same as those in the constant-speed viscometer. In the newer unit, heating tape was placed around the bottom supports of the reservoir to compensate heat losses by conduction through this heavy metal part. This heater, which was controlled through a variable transformer, eliminated any cold end effects, and careful measurements showed that a uniform temperature was obtained in the polymer melt for at least 7 in. above the orifice.

In operation of the earlier, constant piston-speed unit, the first inch of polymer in the reservoir was extruded and discarded because of the tendency for the orifice end to be cooler. Although temperature control was better in the constant-pressure device, comparison of results below shows that the procedure described effectively eliminated any temperature-related errors in the earlier machine. This is to be expected since polyethylene is a good thermal insulator and extrusion rates were fast enough to prevent equilibration of melt and orifice wall temperatures in the short, colder end of the controlled-speed apparatus.

In both rheometers, the apparent shear stress τ_a is given by

$$\tau_a = PR/2L \tag{1}$$

where P is the pressure signalled by the transducer and R and L are the orifice

radius and length, respectively. The apparent shear rate $\dot{\gamma}_a$ is obtained with the conventional assumption of melt incompressibility as

$$\dot{\gamma}_a = \frac{4(d/t)\pi r^2}{\pi R^3} = \frac{4r^2 d}{R^3 t} \tag{2}$$

where r is the reservoir radius and d is the distance moved by the piston in time t.

Melt density was estimated by an extension of technique described elsewhere[2,3] for a deadweight-driven rheometer. The apparent density ρ is given by

$$\rho = M/\pi d r^2 \tag{3}$$

where M is the mass of polymer extruded in time t. Earlier work[1] has shown that leakage of the polymer into the region between the piston and reservoir wall is negligible.

The polyethylene studied was Marlex 6009, which is a 0.9-melt index, linear polymer from the Phillips Company. Polyethylene granules were milled with 0.2 weight percent 4,4′-thiobis(3-methyl-6-*tert*-butylphenol) at fixed mill roll speeds for 3–5 min. This antioxidant content is sufficient to stabilize the polymer against degradation during extrusion experiments.[1,2]

Specimens for the current experiments were prepared from milled, stabilized polyethylene with a flash-type compression molding procedure.[4] Pressures in this operation were as high as 20,000 psi, and air could be effectively squeezed out of the polymer by molding plaques in a ⅛-in. steel frame. These plaques were then die-punched into discs for loading the rheometer. These discs were slightly undersized, compared to the reservoir area, to facilitate release of air when the discs were stacked to obtain the required height of polymer in the barrel.

Gas entrapment is eliminated with this technique as evidenced by the absence of voids in the polymer which was extruded from the open reservoir, with base plug and orifice removed, at the end of each experiment.

Both types of rheometer gave apparent melt densities at low shear rates which coincided closely with those from dilatometry or other measurements on static melts.[1–4] Experiments were always started initially with about 8 in. of polymer in the reservoir to normalize any potential time-dependent or drainage effects.[15,16]

Results

A double-valued flow curve can be obtained with linear polyethylene at sufficiently high rates of flow from a reservoir into a narrower orifice. A hysteresis loop is exhibited with two values of mass flow rate (or apparent shear rate) at the same extrusion pressure as the pressure is cycled through the melt fracture region.[12,13] When rheometers are operated in the so-called "constant flow rate" mode, this usually involves use of a piston advancing at a set rate in a polymer-filled reservoir. In this case, a periodic variation of the extrusion pressure with fixed piston speed is observed in a certain shear rate range.[13,17] Thus, a double-valued shear stress is observed at fixed nominal shear rate.

The constant-pressure rheometer produced a conventional flow curve, with hysteresis, for Marlex 6009 at 186.0°C. This is shown in Figure 2. Replicate

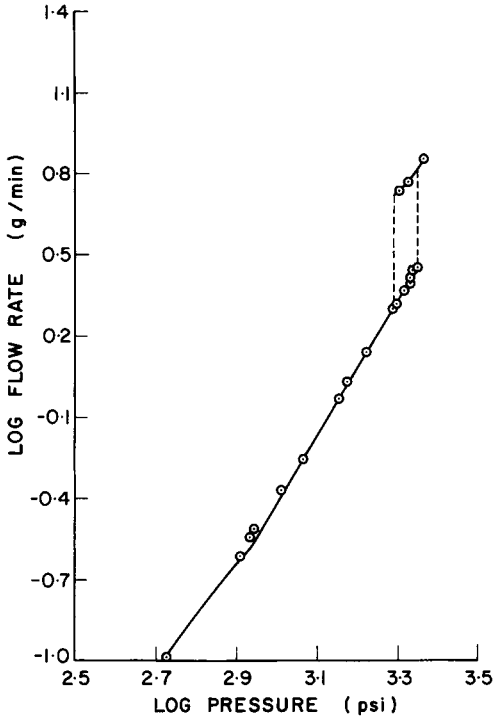

Fig. 2. Mass flow rate vs extrusion pressure in constant-pressure rheometer (186.0°C).

measurements agreed very closely. Apparent densities which were obtained by application of eq. (3) are shown as a function of extrusion pressure in Figure 3. Low-pressure (500–850 psi) values average around 0.762 g/cm^3. The density of this polymer at the extrusion temperature and ambient pressure is near 0.759 g/cm^3,[2,4,18–20] and the compressibility of high-density polyethylene under these conditions is about 1.4×10^{-4} atm^{-1}.[21] Thus, the expected density at 800 psi pressure is near 0.765 g/cm^3, which is within satisfactory agreement of the measured figures.

Marlex 6009 extrudates were well into the melt fracture region at applied pressures near 2500 psi with the particular orifice used in this work. (The exact location of the melt fracture shear stress is not possible because of the hysteresis shown in Fig. 2.) Apparent densities of the polyethylene melt during melt fracture averaged 0.775 g/cm^3, whereas the expected value from the quoted

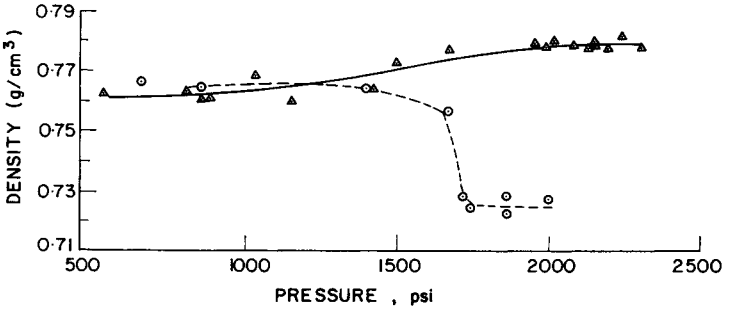

Fig. 3. Apparent density of Marlex 6009 at 186°C. Steel die, L/R = 22.30, R = 0.0391 cm: (▲) constant-pressure; (⊙) constant speed extrusion.

compressibility is 0.778 g/cm^3 under 2500 psi pressure. This is within experimental uncertainty of our measured value.

An ethylene–butylene copolymer (du Pont Canada Sclair 57B, melt index 0.4 and 0.95 g/cm^3 nominal density at room temperature) was also studied in the constant-pressure rheometer. Unlike Marlex 6009, this polymer does not exhibit a double-value flow curve. Melt densities of Sclair 57B measured in and near the melt fracture region agreed with those obtained with Marlex 6009 at similar pressures.

Table I records the constant-pressure extrusion data for Marlex 6009. Tabulated standard deviations of density values and die swell figures are mentioned later in the text. Apparent densities of Marlex 6009 were found to be strongly time dependent in constant piston-speed operation.[1] Equilibrium densities at shear rates lower than the instability region are given in Table II, from the paper of Rudin and Vlasschaert.[1] Two of the experiments were with orifices which had slightly different dimensions from those of our standard capillaries, and the apparent shear stress and shear rate were recalculated for these cases from eqs. (1) and (2). The apparent flow curve was not affected by use of steel, brass, or glass capillaries.[1]

Densities in constant piston-speed extrusion are recorded in Figure 3, which also includes constant-pressure data points. The data points for the two extrusion modes overlap at lower flow rates, but the apparent density decreases drastically in constant-speed operation as the melt fracture region is approached. This is not true of constant-pressure operation.

Oscillating flow was prominent in the constant-speed mode with steel capillaries as well as with an aluminum orifice (L/R = 21.28, R = 0.0412 cm) and a brass die (L/R = 21.87, R = 0.0401 cm). The general behavior with these dies is shown in Figure 4. This is as expected in controlled piston-speed operation.[15] Raw data for the brass and aluminum dies are given in Tables III and IV.

It will be seen from these tabulated results that apparent melt densities change drastically as the flow mode oscillates between smooth and rough regions. The apparent densities in the rough regions are sometimes higher than the density of the polymer at room temperature. Since this is physically impossible, these observations indicate that the polymer in the rough mode is flowing faster on a volumetric basis than the rate at which the piston is clearing the barrel. Similarly, in the smooth flow region, the volume of polymer extruded in unit time is less than the cylinder volume cleared by the piston. This is reasonable if the fast flow creates a lower melt density ahead of the piston and part of the subsequent piston advance recompresses the melt. It is interesting in this connection that the mean values of apparent melt density with these two orifices in constant piston-speed extrusion in both rough and smooth modes are 0.776 g/cm^3 (brass) and 0.771 g/cm^3 (aluminum). These values agree with the figure of 0.775 found at comparable extrusion pressures in a steel die in the constant-pressure rheometer.

It is well known that the size of the hysteresis loops in constant-pressure piston extrusion increases with increasing L/R ratio of the capillary.[14] Our constant piston-speed experiments required convenient cycling times so that alternate rough and smooth extrudates could be obtained for density measurements. The orifice length/radius ratio was found to affect this cycling time at a given depth of polymer in the reservoir. Cycling times were inconveniently long with L/R

TABLE I
Data for Constant-Pressure Operation, Marlex 6009, at 186°C[a]

Pressure, psi	Shear Stress,[b] (dynes/cm^2) × 10^{-6}	Shear rate,[b] sec^{-1}	Average density,[c] g/cm^3	Standard deviation of density	Mass flow rate, g/min	Die swell ratio	Extrudate appearance
856	1.32	133.2	0.761	0.019	0.2854	1.74	smooth
877	1.35	142.3	0.761	0.019	0.3052	1.75	smooth
1022	1.58	196.4	0.768	0.0134	0.4250	1.80	smooth
1493	2.31	486.8	0.773	0.016	1.0596	—	smooth
1950	3.01	907.1	0.780	0.006	1.9926	2.14	smooth
2015	3.11	2467.6	0.780[d]	0.002	5.4233	—	rough
2073	3.20	1053.7	0.779	0.009	2.3115	2.18	smooth
2124	3.28	2643.4	0.7769[d]	0.013	5.7774	—	rough
2146	3.31	1174.1	0.780	0.006	2.5811	—	wavy
2146	3.31	1170.1	0.777	0.005	2.5592	2.20	smooth
2189	3.38	1267.8	0.772	0.008	2.7571	—	wavy
2233	3.44	1272.0	0.781	0.006	2.8010	—	wavy
2320	3.58	3244.7	0.778[d]	0.008	7.1100	—	rough
2147	3.31	1120.5	0.778	0.009	2.4645	2.17	smooth
1987	3.06	945.5	0.776	0.008	2.0667	2.12	smooth
1668	2.57	628.3	0.769	0.011	1.3608	2.01	smooth
1428	2.20	425.7	0.764	0.010	0.9156	1.90	smooth
1160	1.79	257.6	0.760	0.019	0.5514	1.83	smooth
808	1.25	112.0	0.764	0.025	0.2408	1.71	smooth
532	0.82	48.0	0.762	0.036	0.1029	1.62	smooth

[a] Steel die, R = 0.0391 cm, L/R = 22.30.
[b] Apparent values.
[c] More than 24 samples were taken to obtain each average density value except those values with superscript (d).
[d] Six sample measurements were taken to obtain the average value.

TABLE II
Equilibrium Densities of Marlex 6009 in Constant-Speed Extrusion[1]

Temp., °C	Pressure, psi	Shear stress,[a] dynes/cm^2	Shear rate,[a] sec^{-1}	Average density,[b] g/cm^3	Standard deviation of density	Mass flow rate, g/min	Die swell ratio
186.3	663	1.02×10^{6}[c]	65.9[c]	0.769	0.011	0.1426	1.75
185.7	852	1.32×10^{6}[d]	86.4[d]	0.765	0.014	0.1866	—
186.8	1392	2.15×10^{6}[e]	329.6[e]	0.764	0.016	0.7093	1.87
186.0	1668	2.57×10^{6}	468.3	0.757	0.007	0.9985	1.96
186.2	1716	2.65×10^{6}	560.8	0.728	0.008	1.1507	1.99
186.2	1740	2.68×10^{6}	584.8	0.725	0.007	1.1941	1.99
185.4	1854	2.86×10^{6}	698.0	0.729	0.003	1.4328	2.03
186.2	1860	2.87×10^{6}	715.6	0.722	0.012	1.4562	2.02
187.5	1998	3.08×10^{6}	845.3	0.723	0.006	1.7209	2.10

[a] Apparent values.
[b] Ten samples were taken to obtain each average density value.
[c] Values obtained with steel die $R = 0.0499$ cm, $L/R = 21.0$.
[d] Values obtained with a glass die $R = 0.0490$ cm, $L/R = 19.3$. Pressure and mass flow rate values listed are adjusted to die $R = 0.0391$, $L/R = 22.30$.
[e] Values obtained with a steel die $R = 0.0391$ cm, $L/R = 22.30$.

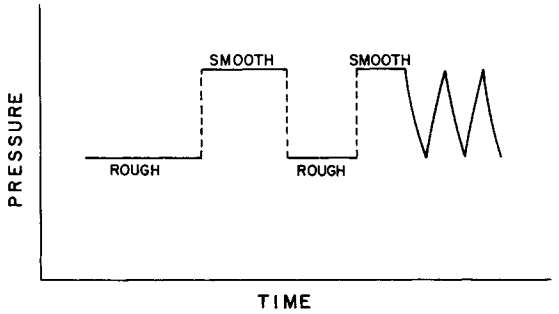

Fig. 4. Schematic of pressure oscillations and extrudate appearance in constant-speed extrusion.

TABLE III
Data for Oscillating Flow Behavior Marlex 6009 at 186.5°C[a]

Extrudate	Pressure,[b] psi	Apparent shear stress, dynes/cm^2	Apparent shear rate, sec^{-1}	Apparent density, g/cm^3	Standard deviation of density	Average mass flow rate,[b] g/min	Distance of piston travel, in.
Rough	1789	2.78×10^6	1052.3	0.981	0.043	2.907	0.30
Smooth	2080	3.22×10^6	987.3	0.601	0.024	1.672	0.30
Rough	1789	2.78×10^6	1287.9	0.898	0.039	3.157	0.30
Smooth	2110	3.27×10^6	1061.3	0.604	0.017	1.807	0.18
Half-half	1957[c]	3.03×10^6	1173.2	0.731	0.018	2.414	0.49

[a] Brass die, $R = 0.0401$ cm, $L/R = 21.87$. Overall average density = $[(0.9808 \times 0.3) + (0.6013 \times 0.3) + (0.8977 \times 0.3) + (0.6044 \times 0.18) + (0.7306 \times 0.45)]/1.57 = 0.7712$.

[b] Values of pressure and mass flow rate are adjusted for the die dimensions of $R = 0.0391$ cm, $L/R = 22.30$.

[c] Average of two oscillating pressures.

= 20.8 dies and were reduced to experimentally convenient values when the L/R ratio was increased to about 22 or slightly higher. Capillaries with L/R ratios of 28 or more produce no melt fracture because the highest shear stress, eq. (1), available within the limits of our pressure transducer was below the actual value for this phenomenon with our polymer.

The flow curves obtained in constant-pressure and constant-speed operations are compared in Figure 5. All values have been adjusted to the dimensions of our standard die [$L/R = 22.30, R = 0.0391$ cm] by application of eqs. (1) and (2) to correct for variation in die dimensions. We note in Figure 5 that the mass flow rate–pressure plots coincide at lower pressures and deviate to a greater extent as the extrusion pressure increases. The constant piston-speed apparatus produces a lower mass flow rate at given extrusion pressure. A slightly higher pressure is observed in the melt in constant piston-speed operation when the data from the two modes are compared at fixed mass flow rate in the region just below the melt fracture region. This reflects the fact that the polymer in the fixed-speed method of extrusion is dilating as it flows toward the die. It has a lower effective density since the reservoir volume is being cleared at the same rate in both extrusion modes. The piston must therefore exert a higher pressure to move the same mass of polymer in given time.

TABLE IV
Data for Oscillating Flow Behavior of Marlex 6009 at 186°C[a]

Extrudate appearance	Pressure, psi	Apparent shear stress, dynes/cm^2	Apparent shear rate, sec^{-1}	Apparent density, g/cm^3	Standard deviation of density	Average mass flow rate, g/min	Distance traveled, in.
Rough	1752	2.84×10^6	1115.0	0.996	0.042	3.661	0.41
Smooth	2022	3.28×10^6	1012.4	0.580	0.021	1.936	0.40
Rough	1798	2.78×10^6	1158.0	0.920	0.046	3.510	0.40
Smooth	1992	3.23×10^6	989.5	0.585	0.040	1.906	0.15
Smooth	1926	3.12×10^6	807.5	0.732	0.007	1.946	0.90

[a] Aluminum die, $R = 0.0412$ cm, $L/R = 21.28$. Overall average density = 0.776 g/cm^3.

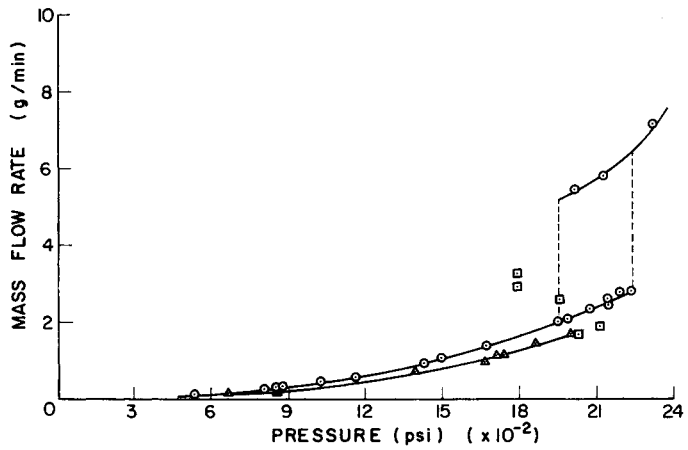

Fig. 5. Mass flow rate of Marlex 6009 vs extrusion pressure relations at 186° with standard die, $L/R = 0.0391$, $R = 0.0391$: (⊙) constant pressure; (▲) constant speed; (⊡) oscillation flow.

The two flow curves are still quite distinct at higher shear rates when the data in Figure 5 are converted to apparent shear stress–apparent shear rate values by application of the equilibrium densities recorded above to convert mass to volumetric flow rates.

Die swell of smooth extrudates was measured with a micrometer after the polymer had frozen. Die swell is recorded here as the quotient of the diameter of the leading end of the frozen extrudate divided by the orifice diameter. Air quenching may affect the results of such determinations, but the data from the two modes of operation are internally consistent. It is clear from Figure 6 that the same die swell was obtained in both modes of operation at equivalent apparent shear rates. These results imply that fixed-speed extrusion will produce extrudates with lower die swell at given apparent shear stress. The difference expected is not large enough, however, to be significant compared to the experimental uncertainty in measurement of die swell of unannealed extrudates.

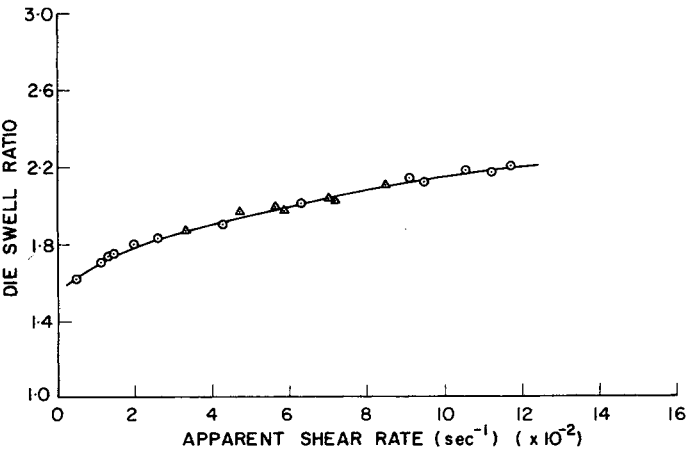

Fig. 6. Die swell of Marlex 6009 as a function of apparent shear rate: (⊙) constant pressure; (▲) constant speed.

PISTON SPEED AND DENSITY FLUCTUATIONS

Density values were calculated from extrudate weights corresponding to a particular distance traveled by the piston. Previous studies with controlled piston speed[1] and with a deadweight load on the piston[2] have produced density figures which fluctuated about the mean value. The present data from controlled-pressure extrusion are similar, and the apparent density figures tabulated here are therefore accompanied by corresponding standard deviation values.

In all cases, the fluctuations in apparent density are in phase with the variations in time for the piston to travel a set distance. This is illustrated in Figures 7 and 8. A previous analysis[1] pointed out that apparent densities of polymer melts are out of phase with piston speed oscillations, although the piston velocity does not enter the density calculations. There would thus appear to be an inverse cause-and-effect relation between the piston speed and apparent polymer density. The slower piston velocities result in a greater mass of polymer extruded

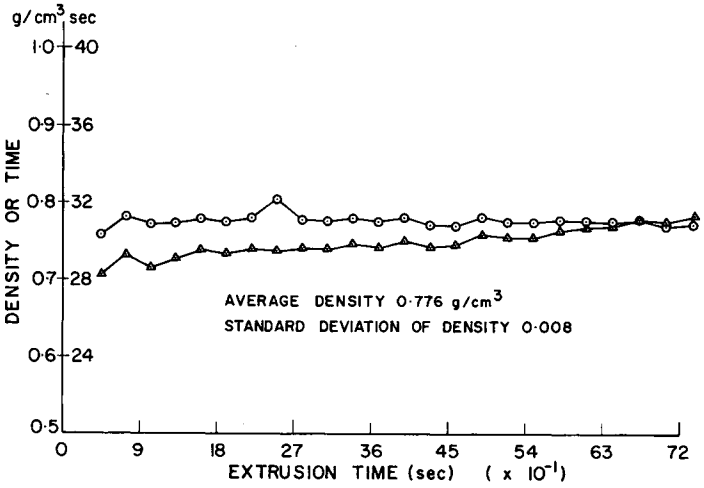

Fig. 7. Simultaneous melt density and time for piston to move 0.1 inch: (⊙) Marlex 6009 density; (▲) piston movement time (0.1 in. along the barrel); pressure 1987 psi.

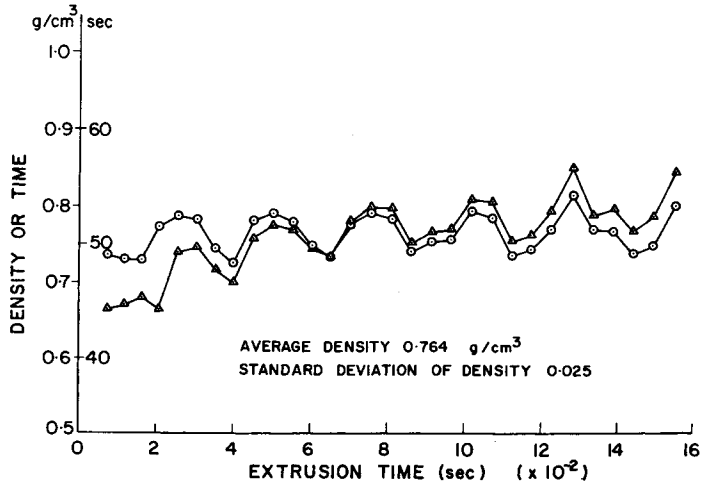

Fig. 8. Simultaneous melt density and time for piston to move 0.2 inch: (⊙) Marlex 6009 density; (▲) time for piston to move 0.2 in. Controlled-pressure extrusion at 808 psi.

per unit volume of the reservoir that is displaced by the piston. A somewhat similar effect has been noted in connection with time-dependent mass flow rates following abrupt changes in extrusion pressure.[15,16]

A mathematical analysis of the data from controlled piston-speed extrusion implies that the polymer melt is not behaving as an incompressible fluid.[1] Variations in plunger speed are acccompanied by successive apparent compressions and decompressions of the polymer melt.

The fluctuations in successive measured densities decreased with increase in piston speed in all extrusion modes and this is consistent with the predictions from a model representing the delayed bulk elasticity of the polymer melt. Reference is made to the article by Rudin and Vlasschaert for details of this model.[1]

The reasons for the fluctuations in piston speed and apparent melt densities are open to speculation. The most obvious triggering mechanism would be a periodic sticking and slipping in the extrusion drive mechanism or rubbing of the piston against the reservoir wall. This seems unlikely, however, because the same general behavior is observed in controlled-speed, controlled-pressure, and deadweight-loaded devices, which differ significantly in drive mechanisms. Great care was taken to ensure the proper alignment of piston and reservoir. Periodic sticking and slipping of the polymer against the die walls is another possible cause of this phenomenon, but this also seems to be unlikely because no significant effects were found with changes in polymer type or in material from which the orifice was constructed.[1]

It seems more probable that the fluctuations noted reflect periodic development and yielding of tensile normal stresses which tend to pull the polymer from the reservoir into the orifice. This mechanism is discussed below in connection with melt fracture.

Han[22] has found pressure fluctuations at the orifice wall at shear rates just below the melt fracture region in extrusion of polystyrene and low- and high-density polyethylene. These fluctuations were most noticeable near the orifice entry. The occurrence of pressure fluctuations in the reservoir as well as in the capillary was interpreted as indicating the absence of wall slippage. These observations seem to be consistent with the density and piston speed fluctuations noted in this work and with the trigger mechanism suggested above.

Pressure fluctuations were not observed in this work as the piston speed varied. One possible reason for this would be that the pressure transducer was sensing the pressure of polymer that is not flowing into the orifice from our very large reservoir. It is also probable that the recorder used was too slow to follow pressure variations.

TIME DEPENDENCE OF MELT DENSITY

The apparent densities of polymer melts are time dependent[1,2] and reflect the previous history of the material for some time after application of a different piston speed or pressure. Similar phenomena were noticed in this work, but no particular attempt was made to follow time trends of density since this behavior was incidental to the main objectivies of this study.

Controlled-pressure extrusion was always started with a relaxed melt, so that effects of prior extrusion could not be studied as was the case in controlled-speed

operations.[1] Figures 7 and 8 record initially low densities and high shear rates (from corresponding piston speeds), as expected. The time to reach equilibrium values decreased with increasing applied pressure, as expected.[15,16] There seem to be no unusual time-dependent features in the present results.

DISCUSSION

Metzger and Hamilton[23] used an Instron[24] constant-speed piston rheometer to study a linear polyethylene and concluded that the melt was incompressible because shear rates calculated from piston speeds corresponded quite well with those obtained by dividing weights of timed extrudates by an assumed melt density equal to 0.76 g/cm^3. We note that the polymer in our work suffered an apparent density decrease of about 6% at the higher shear rates studied. This variation is comparable to the usual uncertainty expected in flow curve measurements. It is highly significant, however, in terms of melt density measurements, as shown by the standard deviations of density recorded here and in an earlier report[1] on the same topic.

The difference in reservoir diameters of the instruments used in the cited work[23] and this study is also probably significant in this connection. Our reservoir has an unusually large diameter for capillary rheometers, and the ratio of reservoir and orifice diameters (r/R) was about 33. Elastic parameters such as die swell, exit pressure, and end corrections[15,25,26] increase with increasing r/R. The work of Metzger and Hamilton was with an r/R ratio of 19, and it is likely that the dilations observed in our work would be less in their experiments, since the polymer melt must develop normal stress differences to account for the density decrease.

We have observed melt density decreases only with high-density polyethylene. Polystyrene and the branched polyethylene mentioned above did not produce detectable apparent melt density decreases at higher shear rates near the melt fracture region. These polymers differ from high-density polyethylene in exhibiting a continuous flow curve through the melt fracture region. The different melt fracture behaviors and melt density–shear rate characteristics can be rationalized as shown below by assuming that the high-density polyethylene melt contains more extensive entanglement networks which can sustain a detectable tensile stress before yielding.

The different flow behaviors in constant piston-speed and constant-pressure extrusions at shear rates below the melt fracture region can be explained in terms of the mechanism suggested earlier[1] to account for the dilation of linear polyethylene melts in fixed piston-speed extrusion. Converging flow of the fluid in the reservoir must result from tensile forces exerted through an entanglement network by the polymer melt in the orifice on material in the larger, upper cavity. The polymer is not only being pushed out of the reservoir by the pressure exerted by the moving piston, it is also being pulled out by the material in the orifice and probably also outside the apparatus. This additional force in the extrusion direction will result in dilation of the melt when the piston is constrained to move at fixed speed, since the flowing polymer adheres to the melt in the circulating so-called "dead spaces" [27] at the bottom of the reservoir and to material nearer to the piston face. This dilation is not evident in constant-pressure extrusion because the piston can accelerate to compensate for the reduced resistance caused

by the tugging action of polymer in the orifice. Mass flow rates at given extrusion pressures are higher in the latter mode since the tensile forces urging the polymer in the reservoir into the orifice are not resisted by the limitations on the rate of advance of the piston.

It should be emphasized that the discussion here does not hinge on whether or not the polymer melt is compressible. There is no doubt that polymer melts can be compressible. The distinction here is between compressible and incompressible *flows*. This work shows that melts with sufficiently highly developed entanglement networks can exhibit density changes in constant piston-speed extrusion from a large reservoir into a small orifice. Compressible flow will not be detectable if the ratios of reservoir-to-orifice diameters are sufficiently small or if the extrusion operation is conducted at fixed pressure on the piston.

The suggested mechanism for compressible flow is consistent with the work of Hürlemann and Knappe,[28] who reported that melt fracture starts when the extensional stress at the die inlet exceeds a critical value. Development of extensional stresses that are transmitted through entanglement networks is essentially the postulate which was invoked to explain the dilation of Marlex 6009 melts in constant piston-speed extrusion.[1] As shown below, this model accounts qualitatively at least for the oscillating flow behavior of linear polyethylene and for the initiation of melt fracture of polymer melts in general.

Everage and Ballman[29] also suggest a tensile failure mechanism, with the onset of melt fracture governed by a critical extensional strain criterion. The present results cannot distinguish between the critical stress[28] and critical strain[29] criteria.

The observed decrease of density of linear polyethylene at higher shear rates below the melt fracture region is believed to be a real effect, in that the melt which is flowing into the orifice has actually dilated. The only other explanation for the reduced ratio of extrudate mass to volume swept out by the piston would be a compression of the melt. This is untenable as a steady flow phenomenon.

The more pronounced time dependence of apparent melt density in constant piston speed than in constant pressure extrusion is also consistent with the postulate that the former flow mode is effectively compressible while the latter is not.

Dilation in constant piston speed extrusion at higher shear rates below the melt fracture region was detected here with linear polyethylene melts, but not with branched polyethylene, polystyrene, or other polymers. This difference parallels the different types of melt flow instability exhibited by these two groups of materials. Discontinuities in the flow curve have been observed at melt fracture only with linear polyethylene and crystalline copolymers of tetrafluoroethylene and hexafluoropropylene.[6] It is suggested here that the triggering mechanism is the same in all cases of melt fracture. Tensile stresses in the axial direction are transmitted through entanglements between the polymer in the orifice and that in the reservoir. When the entanglement network yields under sufficiently high tensile forces, the stressed polymer above the orifice may retract and melt fracture may be observed as a result of the injection of polymer from the "dead spaces" into the flow region.[30] The consequences of melt fracture are different, depending on polymer type, however, because the extent of the entanglement network in linear polyethylene melts is much greater.

Entanglements per se need not necessarily contribute to elastic retraction of the polymer melt when the tensile axial stresses have been released by local yielding of the network. A particular molecule contributes to the elastic network only when it is coupled to at least two other molecules.[31] Linear polyethylene molecules seem to be more highly entangled than polymers with bulkier substituents. When the axial tensile forces become greater than those holding some intermolecular couples together, the remaining elastic network retracts further into the reservoir and the time before reestablishment of a normal flow pattern is greater. Cycling between different modes of flow is thus detectable with linear polyethylene but not with the other polymers we have examined. For similar reasons, dilation at shear rates just below the critical region in controlled piston-speed extrusion can be detected with linear polyethylenes but not with polymer melts with less extensive elastic networks.

As noted above, the dilation measured in controlled piston-speed extrusion at higher shear rates below the critical region is believed to be real. The apparent densities measured during melt fracture cycling in the same extrusion mode are, however, not reflections of the acutal density of the melt in the reservoir. As shown in Table IV, the apparent density of the melt in the fast flow region of the oscillating flow curve is higher than that expected for the solid polymer at the particular extrusion temperature, while the slow flow region is characterized by an apparent density of only 0.6 g/cm^3.

These density figures, from eq. (3), must reflect an alternating situation in which the volume flow rate of the melt is faster and slower than that expected from the piston velocity. This is easily understood in terms of the entanglement model discussed above. Melt fracture is initiated by a local yielding of intermolecular couplings in the wineglass-shaped flow region into the orifice. When this happens, polymer above the break retracts toward the piston, and polymer that is still connected by entanglements to the material in the orifice is pulled out of the reservoir. The flow is faster than it would be if the restraining influence of entanglements to the rest of the polymer melt were still being exerted. This is the fast flow region of the cycle. The apparent density is higher than expected because the mass of polymer extruded in unit time is augmented for the reason given.

It is not possible to measure the actual density of the flowing polymer melt in the oscillating flow region with our equipment because the density is equated through eq. (3) to the quotient of extruded polymer mass to the corresponding volume that was cleared by the piston.

In the slow flow region of oscillating flow, the piston is recompressing the polymer, while normal streamlines are being reestablished. The pressure at the orifice entrances rises during this period and falls when the reestablished axial tensile forces cause another rupture of the entanglement network.

The doubly branched flow curve of linear polyethylene is thus a reflection of the periodic buildup and yielding of elastic axial forces. The elasticity is a reflection of the relatively highly entangled state of the polymer melt. Melt fracture of other polymers is probably triggered by the same mechanism, but their less extensive entanglement networks result in a decreased ability to withstand tensile forces and undetectably shorter intervals between creation and rupture of stressed regions in the melt.

The mechanism suggested is in accord with the controlled piston-speed results

of Myerholtz,[32] who found that the period of load oscillations varied linearly with melt depth. This decreasing period of load oscillation with extrusion time was also observed in this study (Fig. 4). If the detectable period depends, as we have postulated, on the long-range retraction of the linear polyethylene entanglement network, it is evident that this period will be influenced by the volume of polymer melt between the piston face and the orifice.

With fixed melt depth in the reservoir, the load oscillation period passes through a minimum as the plunger velocity increases.[32] This reflects decreasing times needed to reestablish flow streamlines following rupture of the stressed polymer melt. At sufficiently fast plunger speeds, smooth portions of the cycle are not detectable, and linear polyethylene behaves ostensibly like other polymers undergoing melt fracture.

Some controversy exists in the literature regarding the site of initiation of flow instabilities which are variously placed at the die inlet or inside the capillary near the wall, depending on the particular polymer and experimental conditions. Bialas and White[33] have reviewed the literature in this regard up to 1968. The mechanism suggested here involves yielding of an entanglement network under stresses transmitted between polymer in the inlet (or even outside the capillary) and material in the reservoir. It does not seem to be important where this rupture is manifested, as the following discussion shows.

A variety of mechanisms have been proposed for the cause of melt flow instabilities. The model proposed here is an elaboration of one of these (melt fracture) and is shown to account for all the important experimental observations which have been made in this connection.

The triggering mechanism for melt fracture and for oscillating flow behavior of linear polyethylene is believed to be the yielding of an intermolecular network under tension in the flow direction. Melt fracture may be accompanied by flow or pressure oscillations if the intermolecular network is sufficiently extensive and elastic (chains need to be coupled to at least two other chains). The melt fracture need not necessarily occur at a constant shear strain, however. The fundamental parameters here are probably the tensile stress generated in the particular flow and the strength of the melt network. The latter property will depend on the polymer type and molecular weight distribution and also in some cases on the melt history.[31,34,35]

Evidence is contradictory regarding the role of stick-slip polymer flow in melt fracture. Benbow and Lamb[36] extruded silicone gum through transparent acrylic dies and observed what appeared to be slippage at the die wall at shear stresses above the melt fracture point but not below. When the flow in a Woods metal die was stopped at a shear stress in the melt fracture region and then the die was melted, the polymer in the die was found to be distorted and to have undergone very little contraction in length. At lower shear stress, the polymer contraction was appreciable but its surface remained smooth. This difference in axial contraction was attributed to slippage at the wall. It seems equally likely, however, that the polymer produced at low shear stresses contained a stressed melt network while tensile forces in the melt fracture region would have already caused a rupture of the elastic network. The phenomena described could be explained in terms of a yielding of the melt very near to the die wall but not necessarily at the polymer/wall interface.

Cogswell and Lamb[37] studied the periodicity in melt fracture. With regular

wavy extrudates of polypropylene, the mass of polymer per cycle of distortion was found to be proportional to the orifice volume. This implies that the volume of melt involved in a simple melt fracture event occupies the same proportion of the die volume. Although this was explained on different grounds, the effect described is clearly to be expected from yielding of tensile forces exerted by the polymer in the die on that in the reservoir. A broader molecular weight distribution tended to produce a large mass/cycle ratio for equivalent shear stress. This, too, would reflect the existence of longer interconnected melt regions. It was noted also that the mass/cycle ratio increased with increasing L/R ratio of the orifice. This, too, fits the present model, since there will be a larger melt volume below the yield region of the melt network. For constant shear stress, as the piston approaches the die, the mass/cycle ratio decreases. This parallels the observations of Myerholtz[32] noted above in connection with the oscillating flow of high-density polyethylene.

Lupton and Regester[13] studied a high-density polyethylene similar to that used in this work and ascribed oscillating flow to slippage at the die wall. Up to 80% of the shear rate increases at the flow curve discontinuity could be accounted for by the postulate of slippage at the die wall. The same equations would, however, fit a model involving a spurting of the extrudate as a result of failure of the entanglement networks instead of an adhesive failure at the orifice walls.

The birefringence studies of Tordella[14] indicated that the melt flow instability of linear polyethylene and hydrocarbon polymers was initiated within the capillary. Vinogradov and co-workers[58] have also ascribed the melt fracture behavior of branched and linear polyethylene to slip at the capillary wall.

By contrast, den Otter et al.[39,40] found no slippage at the walls of glass slits during flow of high- and low-density polyethylene and of poly(dimethylsiloxane) in the melt fracture region. The report of Maxwell and Galt[41] that wall slippage did occur was thought to be in error because of the large particle sizes of the tracer particles used in this work.

We have found here that the material of construction of the capillary die has no effect on the flow curve of linear polyethylene. Similar results have been reported by others.[14,23,42]

The apparent discrepancy between contradictory observations of conventional linear flow and stick-slip flow seems to have been resolved by Blyler and Hart,[43] who found that the flow curve discontinuity which occurs at the onset of unstable flow may indeed be due to melt slip at or near the capillary wall. However, the velocity gradient within the melt does not undergo any measureable discontinuous change when slip is initiated but continues rather to vary continuously with shear stress. The slip observed with linear polyethylene was shown not to result from adhesive breakdown at the polymer–die interface but more likely in the melt near the wall. It was pointed out that the slip process is governed by the self-adhesion of two layers of polymer melt in close contact and that this self-adhesion is governed by the interpenetration of molecules across the slip interface. This mechanism is evidently consistent with that proposed here for the triggering of melt fracture.

Mention should also be made of Schreiber's[5] authoritative review of the effects of polymer molecular structure on melt flow instabilities. This author points out that the differences in behavior of branched and linear polyethylenes reflect differences in melt elasticity. Although Schreiber's conclusions are stated in

somewhat different terms, his summary accords in general with the hypothesis presented here in that the variations of molecular weight and molecular weight distribution which contribute to hysteresis flow will be those which also produce more extensive elastic networks in polymer melts.

Finally, we note that hole pressure errors resulting from the use of a flush-mounted pressure transducer can be safely ignored in shear stress and viscosity determinations such as those made here.[44]

This work was supported in part by the National Research Council of Canada. This paper was presented in part at the Chicago AIChE meeting, 1976.

References

1. A. Rudin and A. G. Vlasschaert, *Trans. Soc. Rheol.*, **13**, 551 (1971).
2. A. Rudin, K. K. Chee, and J. H. Shaw, *J. Polym. Sci. C*, **30**, 415 (1970).
3. K. K. Chee and A. Rudin, *J. Macromol. Sci.-Phys.*, **B7**, 503 (1973).
4. K. K. Chee and A. Rudin, *Ind. Eng. Chem., Fundam.*, **9**, 177 (1970).
5. H. P. Schreiber, *J. Polym. Sci. B*, **7**, 851 (1969).
6. J. P. Tordella, in *Rheology*, Vol. 5, F. R. Eirich, Ed., Academic Press, New York, 1969, Chap. 2.
7. E. B. Bagley and H. P. Schreiber, in *Rheology*, Vol. 5, F. R. Eirich, Ed., Academic Press, New York, 1969, Chap. 3.
8. J. L. White, *Appl. Polym. Sci. Symp.*, **20**, 155 (1973).
9. J. P. Tordella, *J. Appl. Phys.*, **27**, 454 (1956).
10. E. B. Bagley and H. P. Schreiber, *Trans. Soc. Rheol.*, **5**, 341 (1961).
11. J. Vlachopoulos and S. Lidorikis, *Polym. Eng. Sci.*, **11**, 1 (1971).
12. E. B. Bagley, I. M. Cabott, and D. C. West, *J. Appl. Phys.*, **29**, 109 (1958).
13. J. M. Lupton and J. W. Regester, *Polym. Eng. Sci.*, **5**, 1 (1965).
14. J. P. Tordella, *J. Appl. Polym. Sci.*, **7**, 215 (1963).
15. H. P. Schreiber, *Polym. Eng. Sci.*, **6**, 317 (1966).
16. A. Rudin and H. P. Schreiber, *SPE J.*, **20**, 533 (1964).
17. T. Kataoka and S. Ueda, *Rheol. Acta*, **10**, 446 (1971).
18. M. G. Gubler and A. J. Kovacs, *J. Polym. Sci.*, **34**, 551 (1959).
19. M. J. Richardson, P. J. Flory, and J. B. Jackson, *Polymer (London)*, **4**, 221 (1963).
20. B. W. Terry and K. Yang, *SPE J.*, **20**, 540 (1964).
21. W. Parkes and R. B. Richards, *Trans. Faraday Soc.*, **45**, 20 (1949).
22. C. D. Han and R. R. Lamonte, *Polym. Eng. Sci.*, **11**, 385 (1971).
23. A. P. Metzger and C. W. Hamilton, *SPE Trans.*, **3**, 21 (1963).
24. E. H. Merz and R. E. Colwell, *ASTM Bull.*, **232**, 63 (Sept. 1958).
25. C. D. Han and K. U. Kim, *Polym. Eng. Sci.*, **11**, 395 (1971).
26. N. D. Sylvester, *J. Macromol. Sci. Chem.*, **A3**, 1033 (1969).
27. E. B. Bagley and H. P. Schreiber, *Trans. Soc. Rheol.*, **5**, 341 (1961).
28. H. P. Hurlimann and W. Knappe, *Rheol. Acta*, **11**, 292 (1972).
29. A. E. Everage, Jr., and R. L. Ballman, *J. Appl. Polym. Sci.*, **18**, 933 (1974).
30. H. P. Schreiber, E. B. Bagley, and A. M. Birks, *J. Appl. Polym. Sci.*, **4**, 362 (1960).
31. H. P. Schreiber, A. Rudin, and E. B. Bagley, *J. Appl. Polym. Sci.*, **9**, 887 (1965).
32. R. W. Myerholtz, *J. Appl. Polym. Sci.*, **11**, 687 (1967).
33. G. A. Bialas and J. L. White, *Rubber Chem. Technol.*, **42**, 682 (1969).
34. A. Rudin, *Polym. Eng. Sci.*, **10**, 94 (1970).
35. E. R. Howells and J. J. Benbow, *Trans. Plast. Inst.*, **30**, 240 (1962).
36. J. J. Benbow and P. Lamb, *SPE Trans.*, **3**, 7 (1963).
37. F. N. Cogswell and P. Lamb, *Trans. Plast. Inst.*, **35**, 809 (1967).
38. G. V. Vinogradov and L. I. Ivanova, *Rheol. Acta*, **6**, 209 (1967).
39. J. L. Den Otter, J. L. S. Wales, and J. Schijf, *Rheol. Acta*, **6**, 205 (1967).
40. J. L. den Otter, *Rheol. Acta*, **10**, 200 (1971).
41. B. Maxwell and J. C. Galt, *J. Polym. Sci.*, **62**, S50 (1962).
42. P. L. Clegg, *Rheology of Elastomers*, Pergamon Press, London, 1958.
43. L. L. Blyler, Jr., and A. C. Hart, Jr., *Polym. Eng. Sci.*, **10**, 193 (1970).
44. K. Higashitani and A. S. Lodge, *Trans. Soc. Rheol.*, **19**, 307 (1975).

Received December 14, 1976